

Supporting information

Measurements of Single-Molecule Electromechanical Properties based on Atomic Force Microscope Fixed-Junction Technique

Lei Yu^{*†a,b}, Mingyang Zhang^{†a,b}, Haijian Chen^{a,b}, Bohuai Xiao^{a,b}, and Shuai Chang^{*a,b}

^a *The State Key Laboratory of Refractories and Metallurgy, Wuhan University of Science and Technology, Wuhan, Hubei 430081, China*

^b *The Institute of Advanced Materials and Nanotechnology, Wuhan University of Science and Technology, Wuhan, Hubei 430081, China*

† These authors contributed equally.

* E-mail: schang23@wust.edu.cn, yuleiest@163.com

Contents

S1. Experimental

S1.1 Preparation of gold-coated AFM tip

S1.2 Substrate preparation

S1.3 AFM-FJ measurements

S2. Analysis of AFM-FJ data

S2.1 Data analysis

S2.2 Molecular junction stretch length

S2.3 Fitting process of force events

S2.4 Two-dimensional universal force traces for HDA and HDT.

References

S1. Experimental

S1.1 Preparation of gold-coated AFM tip

Gold-coated AFM tips are fabricated by sequentially evaporating 20nm Cr and 80nm Au with a thermal evaporation system (Covap, Angstrom Engineering, Canada) on commercial Si₃N₄ AFM probes (Tap300Al-G, Budget Sensors, Bulgaria) which are cleaned with plasma. The Au layer serves as the conductive surface and the Cr layer improves the adhesion of Au to Si₃N₄.

S1.2 Substrate preparation

The Au substrate is fabricated by depositing 100 nm Au on a fresh-cleaved mica substrate. The molecules for conductance measurements were purchased from TCI (Shanghai, China). Ethanol was purchased from Sinopharm Chemical Reagent (Shanghai, China). All chemicals were used without further purification. The thiol linker molecules (HDT and ODT) were dissolved and diluted in ethanol to a final concentration of 0.05 mM. The amine linker molecules (HDA and ODA) were dissolved and diluted in ethanol to a final concentration of 1 mM. Before functionalization, the Au substrate is flame annealed with hydrogen to remove organic residues. It is then immersed in the molecular solution for 30 s (HDT and ODT) or 1 h (HDA and ODA). Before usage, the samples were rinsed with ethanol and blown dry with argon gas.

S1.3 AFM-FJ measurements

AFM-FJ is a characterization mode for simultaneously measuring the mechanical and electrical properties of a single molecule in a combined platform of AFM and scanning tunneling microscopy (STM). AFM-FJ measurements were carried out in a commercial scanning probe microscope (Keysight SPM 6500, USA) under ambient condition. The gold-coated AFM tip was first approached to the substrate surface with a gap distance of about 0.3-0.5 μ m in an AFM contact mode, and further approached to the surface to reach the setpoint current under STM constant current mode with an applied sample bias at 0.1 V. Once engaged, the tunneling current through the two gold electrodes and the force applied on the AFM cantilever probe (calculated by multiplying the deflection of the cantilever with its spring constant¹), as well as the z-direction movement of the piezoelectric positioner are recorded simultaneously (See Fig. 1B in the manuscript). Because the tunneling current is extremely sensitive (exponentially) to the gap distance, the gap distance can be controlled with a precise resolution. In fixed junction technique, the gap distance between two electrodes is kept constant by setting a fixed preset setpoint current in a constant current mode. The setpoint current was selected to be 1 nA for shorter molecules (HDA and HDT) and 0.2 nA for longer molecules (ODA and ODT). The estimated gap distance at such selected setpoint current is close to the length of the measured molecule, as calibrated in our previous conductance measurements using FJ and MJM techniques.^{2,3} In this way, the well-defined nanogap promotes an increased formation rate of molecular junctions and offers an optimized gap condition for studying the electrical properties of single molecules. During the AFM-FJ measurement, the servo I gain was

set at 0.1 and P gain was set at 0, which were carefully selected to prevent slow drift of baseline current and have little effect on the current spikes. In contrast to the commonly used break junction (BJ) technique, the FJ technique doesn't require contacts between electrodes, which gives some advantages in maintaining the consistency of electrode conformations and local environmental conditions at the nanoscale.

The typical spring constant of the commercial AFM tip is 40 N/m, and the spring constant for individual AFM tip is calibrated by thermal noise method⁴ after AFM-FJ measurement, ranging from 33.7 N/m to 46.1 N/m in our experiments.

S2. Analysis of AFM-FJ data

S2.1 Data analysis

For each molecule, the data of time traces over 1.5 hours are collected and analyzed. When a single molecule is bridging between two electrodes, current jumps appear, with corresponding changes occurring in the position of the piezoelectric positioner and AFM cantilever probe recorded simultaneously, as shown in Fig. 1B. Each current jump is counted as an event for molecular binding. The histogram events are 82 for HDA, 71 for ODA, 88 for HDT, and 283 for ODT. In most cases where no binding events are detected, the gap distance is fixed, and the tunneling current and AFM tip deflection are stabilized, as shown in Figure S1.

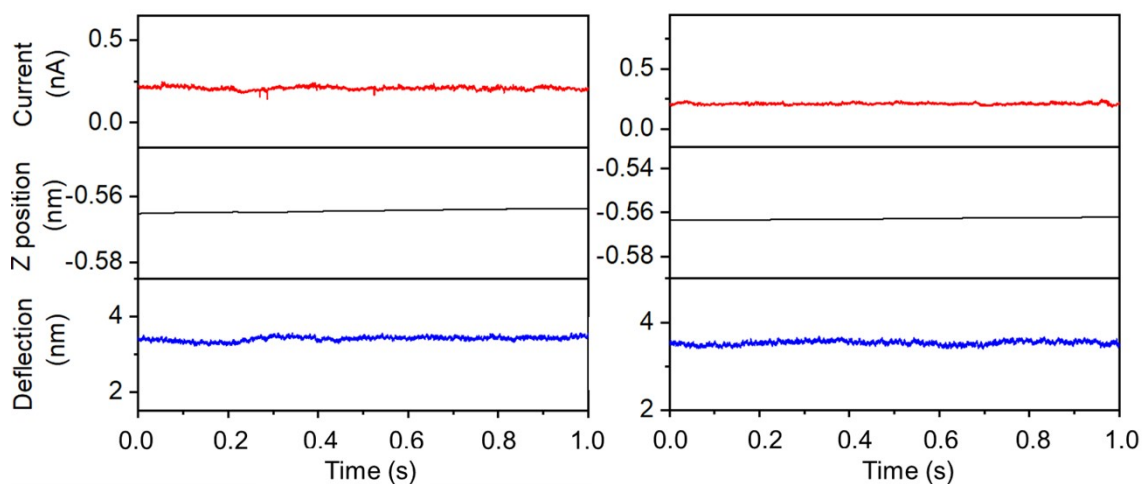


Figure S1. Typical time traces of ODT without current spikes.

Table S1. Analysis of variance (ANOVA) of the rupture force data for four molecules.

Source of Variation	Sum of squares	Degree of freedom	Mean Squares	F	P-value	F crit
Between Groups	21.24843	3	7.082811	14.41228	4.94E-09	2.622046
Within Groups	255.5502	520	0.491443			
Total	276.7986	523				

To better clarify the difference between rupture force data for four molecules, we performed the

analysis of variance (ANOVA) of the rupture force data for four molecules. As shown in Table S1, the P-value between different groups is 4.94×10^{-9} , which is much smaller than the significance value α ($=0.05$). It indicates that there is significant difference between force data for four molecules.

S2.2 Molecular junction stretch length

A more specific schematic diagram of AFM-FJ approach is shown in Figure S2. The molecular junction stretch length (L) can be obtained from the moving distance of piezoelectric tube (Z) minus the tip deflection length change (D).

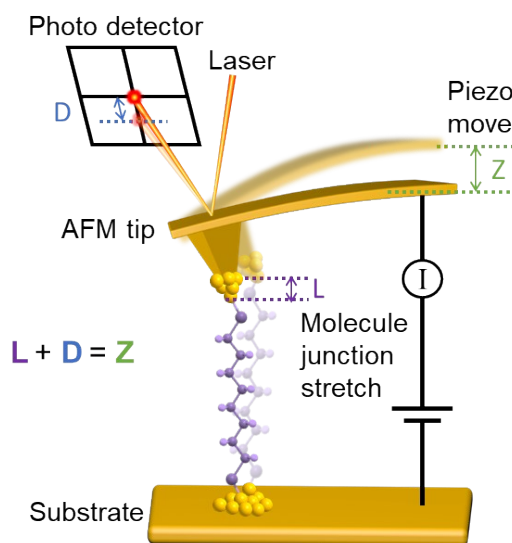


Figure S2. Schematic diagram of AFM-FJ measurement where the molecular junction stretch length (L), the deflection change of laser (D), and the moving distance of piezoelectric tube (Z) are marked in different colors.

S2.3 Fitting process of force events

The hybrid model for force trace fitting can be derived by applying some boundary conditions on the potential of two segments.⁵

The harmonic segment of potential is:

$$U_{harm}(x) = \frac{1}{2}K_{harm}(x - x_0)^2 + U_0 \quad (1)$$

And the logistic segment of the potential is:

$$U_{log}(x) = D / \left(1 + e^{-\frac{(x - x_{Fmax})}{r}} \right) \quad (2)$$

K_{harm} is the stiffness characterizing the harmonic region of the energy profile, whereby x_0 and U_0 are the equilibrium position and energy minimum. Parameters D and r control the overall energy

magnitude and energy scaling with displacement for the logistic region, in which x_{Fmax} describes the position of the force maximum.

To connect these two segments, (a) the logistic segment must pass through the harmonic potential minimum, which requires $U_{harm}(x_0) = U_{log}(x_0)$. (b) The curves join at a displacement where $U = D/4$, which requires $U_{harm}(x_1) = U_{log}(x_1) = D/4$. And (c) the derivative of the logistic and harmonic segments must coincide at this same connection point x_1 . These boundary conditions give three equations to reduce the physical parameters to D and r .

By applying the above conditions, we can get the binding energy:

$$E_{bind} = 0.9687 \times D \quad (3)$$

and the binding length scale:

$$L_{bind} = 3.4310 \times r \quad (4)$$

For the fitting of force data, we use the first derivative of the logistic segment potential versus displacement x as fitting model. That is:

$$\frac{dU_{log}}{dx} = \frac{D}{r} \frac{e^{-(x-x_{Fmax})/r}}{(1 + e^{-(x-x_{Fmax})/r})^2} \quad (5)$$

To fit our AFM-FJ data, we need to replace the time axis of force trace with displacement (Z position in Fig. 1), and follow a three-step fitting procedure. First, D and r are calculated from the rupture force F_{max} and stiffness K_{harm} ($= F_{max}/\Delta Z$) with the formulas below:

$$F_{max} = \frac{D}{4r} \quad (6)$$

$$K_{harm} = \frac{0.0804 \times D}{r^2} \quad (7)$$

And the first fitting (Figure S3, fitting 1) is performed by constraining D , and x_{Fmax} is obtained ($x_{Fmax,1}$). Then the second fitting (fitting 2) is performed by constraining r , and x_{Fmax} is also obtained ($x_{Fmax,2}$). Finally, fitting 3 is performed by constraining x_{Fmax} (average of $x_{Fmax,1}$ and $x_{Fmax,2}$), and the final D and r are obtained. Then E_{bind} and L_{bind} can be acquired from Eqs. 3 and 4 for each experimental trace.

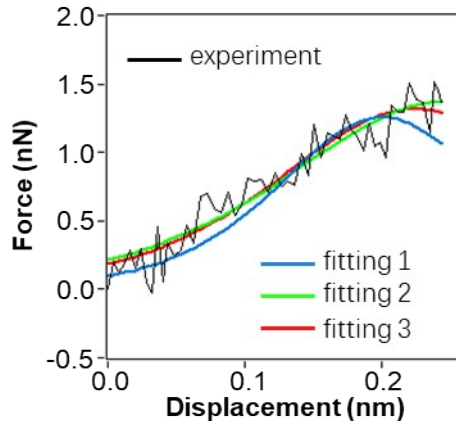


Figure S3. Typical fitting process of the force extension curve based on the model. The adjusted R-square is 0.83 for fitting 1, 0.91 for fitting 2, and 0.90 for fitting 3.

S2.4 Two-dimensional universal force traces for HDA and HDT.

To construct the two-dimensional force map, the force and displacement data were normalized by F_{max} and L_{bind} , respectively. And the displacement of each trace was shifted to zero at the fitted x_{Fmax} . By overlaying hundreds of scaled force traces, the two-dimensional (2D) distributions of four molecules can be constructed as shown in Fig. 3C, D and Fig. S4. And the force profile (black line in Fig. S4) is determined from the hybrid model where harmonic and logistic segments meet at a well-defined connection point as described in S2.3.

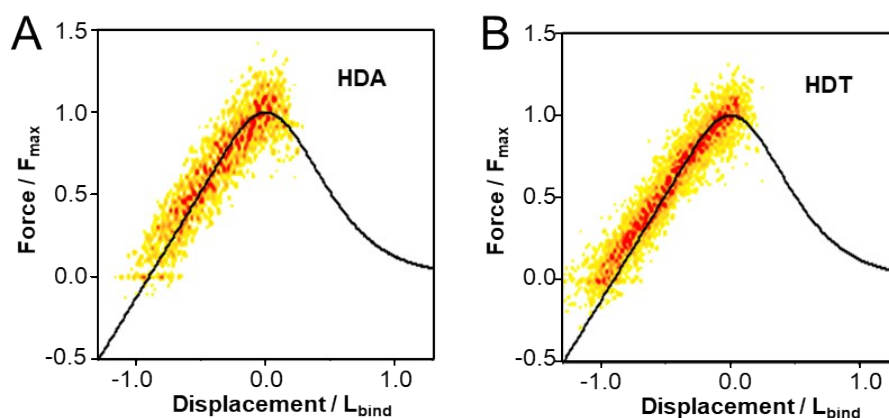


Figure S4. Two-dimensional distribution of the scaled force traces and the corresponding hybrid model fitting curve (black curve) for HDA (A) and HDT (B).

References

1. D. Sarid, Scanning Force Microscopy: With Applications to Electric, Magnetic, and Atomic Forces, 2nd ed. *Oxford University Press*, New York, 1994.
2. B. Xiao, F. Liang, S. Liu, J. Im, Y. Li, J. Liu, B. Zhang, J. Zhou, J. He and S. Chang, *Nanotechnology*, 2018, 29, 365501.
3. H. Chen, Y. Li and S. Chang, *Anal Chem.*, 2020, 92, 6423-6429.
4. J. L. Hutter and J. Bechhoefer, *Rev. Sci. Instrum.*, 1993, **64**, 1868-1873.
5. S. V. Aradhya, A. Nielsen, M. S. Hybertsen and L. Venkataraman, *ACS nano*, 2014, 8, 7522-7530.